

Third-order elastic coefficients and logarithmic strain in constitutive and finite element modelling of anisotropic elasticity

Paweł Dłużewski, Marcin Maździarz, Piotr Tazowski
Institute of Fundamental Technological Research (IPPT PAN)
ul. Pawińskiego 5^B, 02-106 Warszawa, email: pdluzew@ippt.pan.pl

June 8, 2021

Abstract

Third-order elastic coefficients (TOECs) have been measured experimentally and tabulated with pretty good accuracy since the middle of the previous century. In the classical acoustic measurement method the recalculation of instantaneous stiffness change onto TOECs is based on the use of Green strain. In recent calculations performed by means of atomistic and quantum methods many different strain measures are employed. In result, quite different sets of TOECs can be obtained for the same material. In this paper, it is shown how dramatically the coefficients obtained depend on the choice of strain measure. The known formulas for calculation of the second derivative of a tensor-valued function of tensor variable are corrected. The formulas are essential for the correct analytic calculation of the tangent stiffness matrix in finite element method, among others.

Keywords: Third-order elastic coefficients, Logarithmic strain, Anisotropic hyperelasticity, Nonlinear elasticity, Finite deformations, Finite element method

1 Introduction

Recently, the classical second-order elastic constants (SOECs) as well as the higher-order elastic coefficients are more and more often predicted theoretically on the basis of quantum calculations [9, 26, 30, 35, 48, 55–57, 60]. Over many years the elastic coefficients were measured mainly by means of acoustic measurement methods. Thanks to such measurements the second- and third-order elastic coefficients have been tabulated *with pretty good accuracy* for the most of known crystal structures. Despite so large database of TOECs collected over many years, still every year tens of new papers presenting TOECs for known and novel materials are published in journals of solid physics.

It is worth mentioning that *anisotropic* hyperelastic models fitted to TOECs compose only a very small subset among numerous constitutive models describing the anisotropic elastic behaviour of solids. In continuum mechanics a term *nonlinear elasticity* is often identified not with the quantitative modelling of elastic softening or hardening but with a modelling in the limits of finite elastic deformations. Potentially, most of such obtained models can be fitted to the experimentally determined TOECs. Nevertheless, it is easy to note that these two groups of papers develop rather separately. The present paper is situated on the border of these two groups.

Constitutive models of elastic materials should have two fundamental properties:

- First of all, such models should hold the energy balance for an arbitrarily chosen elastic deformation loop. Unfortunately, many of elastic models ignore this fundamental rule. This concerns most of so-called Cauchy elastic materials for which the constitutive relationship is stated directly between the stress and strain measures, see [4]. A similar problem does concern the linear elasticity. Despite that a linear theory is regarded as a theory which does not distinguish the Lagrangian and Eulerian configurations (small strain approach), the correct integration of elastic work done should take into account the change of elastic body shape. As a matter of fact, for each of deformation problem the linear theory of elasticity can be used to obtain two mutually different analytic solutions for displacement vector field derived alternatively from the Lagrangian or Eulerian configuration. For example, the most of analytic solutions applied in civil engineering satisfy the boundary conditions assumed in the Lagrangian configuration. Contrary to civil engineering, almost all of the analytic solutions available in the linear theory of dislocations satisfy the boundary conditions imposed in the Eulerian configuration, cf. e.g.

Eqs (3-45) and (3-46) in [25]. The elastic spring back of such a self-stressed structure leads to quite different analytic function for displacement vector derived from the Lagrangian configuration being then a single- or a multi-connected region of a perfect lattice, cf. [7].

- A second but no less important issue is that the nonlinear elastic behaviour of constitutive models should be in agreement with the nonlinearity demonstrated by real materials. For example, the best-known *anisotropic* Hookean based on Green strain demonstrates a very strong change of instantaneous stiffness. Unfortunately, this elastic hardening runs in the quite opposite direction than those demonstrated by real materials. Namely, according to the experimental evidence, *the instantaneous stiffness of crystals increases strongly under compression and decreases under tension*. This phenomenon is responsible for many physical effects. For example, the experimentally observed sensitivity of elastic stiffness on the applied stress has been used in commercial devices for detection of the residual stresses by means of acoustic waves [6, 11, 15, 46]. Another domain of research in which TOECs play an important role is optoelectronics. Namely, a GPa stress assisting the lattice mismatch between monolayers in semiconductor devices often results in a strong piezoelectric effect. This effect shifts the band gap in quantum structures and changes their optical properties, cf. [17, 34]. Recently, the effect of the higher order elastic and piezoelectric coefficients on the optical properties of quantum dots is calculated numerically, see e.g. [31, 32]. Another example concerns the nonlinear elastic effect induced by dislocations. Due to the asymmetry in the stress/strain response for the extension and compression, the nonlinear theory of crystal defects predicts the volume expansion induced by edge dislocations and other extended defects, see [25, 27, 50]. TOECs are used also for prediction of elastoplastic behaviour of materials undergoing megabar pressures up to 300 GPa [8, 16, 42]. In geophysics, an isothermal Eulerian Birch–Murnaghan equation of state is used despite of the recognized shortcomings for large compressive strains [1, 41]. Poirier et al. [45] have shown that the analogical state equation for strain energy constructed from logarithmic (Hencky) strain is more stable than the traditional Eulerian Birch–Murnaghan equation based on the use of Green strain.

The awareness of a strong dependency of TOECs on the choice of strain measure, could be the reason why Thurston et al. already in 1966 named TOECs not *constants* but only *coefficients*. Since that time, TOECs have been successfully determined by measuring the dependency of elastic wave speed on the stress applied to crystal structures [3, 12, 20, 22, 29, 33, 49, 51, 53, 54]. Despite the fact that the measurement of higher order elastic coefficients of this kind has a long tradition, it appears occasionally that some formulas used through so many years and settled down as a classic are not quite correct. For example recently, the formulas for the extraction of pressure coefficients derived by McSkimin and Andreatch in 1972 [38] were corrected by Winey et al. [58]. In the present paper a similar situation is shown with the formulas for the second order derivative of a tensor-valued function of a symmetric second-order tensor.

In the next section the deformation and strain measures used in the linear and finite deformation theories of elasticity are discussed in brief. Special attention is focused on the strict mathematical relationships between so called linear strain measures and finite strain measures related to mutually different reference configurations. In the mentioned section the known formulas for calculation of the second derivative of a tensor-valued function of tensor variable are corrected. Section 3 is devoted to anisotropic hyperelastic models in which TOECs are used to fit the behaviour of constitutive models to the anisotropic elastic behaviour of real materials. The effect of strain measure on the resultant elastic hardening of Hookian models is discussed in terms of experimentally determined elastic hardening data. This hardening is quantified by means of TOECs fixed experimentally in relation to an arbitrary chosen strain measure. With respect to the revision of the formulas mentioned above, in Section 4 the revised formulas are used for calculation of tangent stiffness matrix in finite element method.

2 Deformation measures

In continuum mechanics two main approaches to the modelling of elastic body are applied. In the linear approach, the body motion is described by means of a displacement vector function that depends either on the reference position or the spatial position of a material particle. Contrary to that, in nonlinear theories the current position \mathbf{x} of the material particle is assumed to be a function of the reference position, $\mathbf{x} = \mathbf{x}(\mathbf{X})$. In such a case, \mathbf{x} and \mathbf{X} are treated as points given by means of curvilinear coordinates on a differential manifold. Neglecting some special cases like the continuum theory of discrete dislocations, the mentioned mapping is assumed to be regular and reversible which means that in most cases an inverse function $\mathbf{X} = \mathbf{X}(\mathbf{x})$ is assumed to be regular and invertible. The last approach based on the use of manifolds is found to be more general with respect to the possibility of considering the deformation of an elastic body in a curvilinear space where a displacement vector field of the same order as of the order of the manifold may not exist. In the present paper, we consider finite deformation of elastic body by means of curvilinear coordinates

embedded in a 3D Euclidean space. In more general case, the analytic relations presented here can be easily translated to an arbitrary 3D Riemannian manifold on which a parallel connection is additionally determined.

Taking into account that $\mathbf{X} = \mathbf{x} - \mathbf{u}$, the *mutually reversible* relationship can be rewritten in the form

$$\mathbf{F} = (\mathbf{1} - \nabla \mathbf{u})^{-1} = \mathbf{1} + \widehat{\nabla} \mathbf{u}, \quad \nabla \mathbf{u} = \mathbf{1} - \mathbf{F}^{-1}, \quad \widehat{\nabla} \mathbf{u} = \mathbf{F} - \mathbf{1}, \quad (1)$$

where $\mathbf{F} = \frac{\partial \mathbf{x}}{\partial \mathbf{X}}$, $\mathbf{F}^{-1} = \frac{\partial \mathbf{X}}{\partial \mathbf{x}}$; and $\mathbf{1}$ denotes the second order unit tensor.

According to the theorem of polar decomposition, the deformation gradient can be decomposed into the orthogonal tensor of rotation, \mathbf{R} , and the right or left stretch tensors, respectively

$$\mathbf{F} = \mathbf{R}\mathbf{U} = \mathbf{V}\mathbf{R}. \quad (2)$$

Contrary to that, in the linear theory, the displacement gradient is decomposed into an antisymmetric rotation tensor, \mathbf{w} , and symmetric strain tensor, $\boldsymbol{\varepsilon}$, referred alternatively to the Eulerian (spatial) or Lagrangian (reference) configurations,

$$\nabla \mathbf{u} = \mathbf{w} + \boldsymbol{\varepsilon}, \quad \widehat{\nabla} \mathbf{u} = \widehat{\mathbf{w}} + \widehat{\boldsymbol{\varepsilon}}, \quad (3)$$

where

$$\mathbf{w} \stackrel{df}{=} \frac{1}{2}(\partial_{\mathbf{x}} \mathbf{u} - \partial_{\mathbf{x}}^T \mathbf{u}), \quad \boldsymbol{\varepsilon} \stackrel{df}{=} \frac{1}{2}(\partial_{\mathbf{x}} \mathbf{u} + \partial_{\mathbf{x}}^T \mathbf{u}), \quad (4)$$

$$\widehat{\mathbf{w}} \stackrel{df}{=} \frac{1}{2}(\partial_{\mathbf{X}} \mathbf{u} - \partial_{\mathbf{X}}^T \mathbf{u}), \quad \widehat{\boldsymbol{\varepsilon}} \stackrel{df}{=} \frac{1}{2}(\partial_{\mathbf{X}} \mathbf{u} + \partial_{\mathbf{X}}^T \mathbf{u}), \quad (5)$$

the displacement vector function is treated then as a composite vector function $\mathbf{u} = \mathbf{f}(\mathbf{x}(\mathbf{X}))$ or $\mathbf{u} = \widehat{\mathbf{f}}(\mathbf{X})$, respectively. A linear theory of elasticity is often regarded as a theory that by definition ignores any difference between the reference and spatial configuration of elastic body. As a matter of fact, in practical uses, the analytic solutions of boundary-value problems obtained by means of the linear theory can be divided into two separated groups that satisfy the imposed symmetry (loading, kinematic constraints, boundary conditions) in the reference or spatial configurations, alternatively. For example, in the linear theory of dislocations, almost all the known analytic solutions for stress-strain fields have been obtained for the Eulerian configuration. In such a case, in order to find the reference position of a material particle in the Lagrangian configuration the displacement vector field must be pulled back from the Eulerian configuration, cf. the analytic solutions for dislocations in [25]. Recently, the lack of analytic solutions for the displacement vector field related directly to the Lagrangian configuration poses some problem in the use of analytic formulas for the preprocessing of atomistic models of dislocation networks in noncrystalline heterostructures, cf. [7, 59].

Example To illustrate the problem of inaccuracies in the determination of strain with the use of linear strain measures, let us consider two different gradients of displacement vector

$$[\nabla \mathbf{u}_1] = \begin{bmatrix} \frac{1}{2} & \frac{\sqrt{3}}{2} & 0 \\ -\frac{\sqrt{3}}{2} & \frac{1}{2} & 0 \\ 0 & 0 & 1 \end{bmatrix}, \quad \begin{bmatrix} -\frac{1}{2} & \frac{\sqrt{3}}{2} & 0 \\ -\frac{\sqrt{3}}{2} & -\frac{1}{2} & 0 \\ 0 & 0 & 1 \end{bmatrix} = [\nabla \mathbf{u}_2]. \quad (6)$$

From the view point of linear theory the additive decomposition into antisymmetric and symmetric parts gives

$$[\boldsymbol{\varepsilon}_1] = \begin{bmatrix} -\frac{1}{2} & 0 & 0 \\ 0 & -\frac{1}{2} & 0 \\ 0 & 0 & 0 \end{bmatrix}, \quad \mathbf{w}_1 = \begin{bmatrix} 0 & \frac{\sqrt{3}}{2} & 0 \\ -\frac{\sqrt{3}}{2} & 0 & 0 \\ 0 & 0 & 0 \end{bmatrix} = \mathbf{w}_2, \quad \begin{bmatrix} \frac{3}{2} & 0 & 0 \\ 0 & \frac{3}{2} & 0 \\ 0 & 0 & 0 \end{bmatrix} = [\boldsymbol{\varepsilon}_2]. \quad (7)$$

From the viewpoint of finite deformation theory the substitution of (6) into (1b) gives the following matrix representations of deformation gradient

$$[\mathbf{F}_1] = \begin{bmatrix} \frac{1}{2} & -\frac{\sqrt{3}}{2} & 0 \\ \frac{\sqrt{3}}{2} & \frac{1}{2} & 0 \\ 0 & 0 & 1 \end{bmatrix}, \quad \begin{bmatrix} -\frac{1}{2} & -\frac{\sqrt{3}}{2} & 0 \\ \frac{\sqrt{3}}{2} & -\frac{1}{2} & 0 \\ 0 & 0 & 1 \end{bmatrix} = [\mathbf{F}_2]. \quad (8)$$

One can check that these two mutually different deformation gradients are nothing more than two rigid rotations around z axis through the angles $\frac{\pi}{6}$ and $\frac{5\pi}{6}$, respectively. For a rigid body rotation, the strain tensors should vanish. Thus, the non-zero components of linear strains $[\boldsymbol{\varepsilon}_1]$ and $[\boldsymbol{\varepsilon}_2]$ represent only errors generated by the linear theory. As a matter of fact, the anti symmetric tensors $\mathbf{w}_1 = \mathbf{w}_2$ do not distinguish these two quite different rotations.

One of important consequence of the inaccurate determination of strain in linear theories is the incorrect determination of strain energy — independently of whether the elastic strain is very small or not. We do not discuss here which level of linear elastic strain is a sufficiently small to neglect the perpetual motion of such elastic models on deformation loops. The important here is that the mathematical dependency of linear strain measures on rigid rotation makes impossible the measurement of many material coefficients with the use of these strain measures. This concerns TOECs as well as many other coefficients like the second and higher order piezoelectric and magnetostriction coefficients.

2.1 Logarithmic strain measure based on polar decomposition

According to the spectral decomposition theorem the right stretch tensor can be decomposed into three real and positive eigenvalues, u_1, u_2, u_3 , and three unit eigenvectors $\mathbf{u}_1, \mathbf{u}_2, \mathbf{u}_3$, which can be used for the following decomposition of the stretch tensor

$$\mathbf{U} = \sum_{n=1}^3 u_n \mathbf{u}_n \otimes \mathbf{u}_n, \quad (9)$$

where \otimes denotes the dyadic product.

Definition By a Lagrangian strain measure we mean a tensor-valued isotropic function of the right stretch tensor,

$$\widehat{\boldsymbol{\varepsilon}} \doteq \sum_{n=1}^3 f(u_n) \mathbf{u}_n \otimes \mathbf{u}_n, \quad (10)$$

where $f(\cdot)$ is an arbitrarily chosen, sufficiently smooth and monotonically increasing function $f(x) : \mathbb{R}^+ \ni x \rightarrow f \in \mathbb{R}$ which satisfies the conditions: $f(x)|_{x=1} = 0$ and $\frac{df(x)}{dx}|_{x=1} = 1$.

In this definition \mathbb{R} and \mathbb{R}^+ denotes the sets of real and positive real numbers, respectively. This definition includes among others the well-known Seth-Hill family of strain measures defined as

$$\widehat{\boldsymbol{\varepsilon}} \doteq \begin{cases} \frac{1}{m}(\mathbf{U}^m - \mathbf{1}) & \text{for } m \neq 0, \\ \ln \mathbf{U} & \text{for } m = 0, \end{cases} \quad (11)$$

For $m = 2, 1, 0$ and -2 the Green, Biot, logarithmic (Hencky) and Almansi strain measures are obtained, respectively. For a uniaxial stretch test, these family of strain measures was gathered into a common formula by Seth [47] in 1964. In 1970 Hill [23] first applied a definition of an analytic function of a matrix for generalization the Seth's definition to a 3D case. As a matter of fact, functions of matrices have been studied for as long as matrix algebra itself [18, 21]. Indeed, in his seminal *A Memoir on the Theory of Matrices* (1858), Cayley investigated the square root of a matrix, and it was not long before definitions of $\mathbf{f}(\mathbf{U})$ for general \mathbf{f} were proposed by Sylvester and others, see Higham [21]. Seth-Hill family of strains by no means fulfils all possible measures of (10), cf. [10].

As shown by Hill [24], the material derivative of (10) reads

$$\dot{\widehat{\boldsymbol{\varepsilon}}} = \widehat{\boldsymbol{\mathcal{A}}} : (\mathbf{R}^T \mathbf{dR}), \quad \text{where} \quad \mathbf{d} \doteq \frac{df}{2} [\dot{\mathbf{F}}\mathbf{F}^{-1} + (\dot{\mathbf{F}}\mathbf{F}^{-1})^T]. \quad (12)$$

In the eigenvector basis $\{\mathbf{u}_k\}$ the fourth-order proper-symmetric tensor $\widehat{\boldsymbol{\mathcal{A}}}$ is represented by the following non-vanishing components [13]

$$\widehat{\mathcal{A}}_{ijij} = \widehat{\mathcal{A}}_{ijij} = \begin{cases} u_i f'(u_j) & \text{for } i = j, \\ \frac{1}{2} u_i f'(u_j) & \text{for } u_i = u_j \text{ and } i \neq j, \\ \frac{u_i u_j [f(u_i) - f(u_j)]}{u_i^2 - u_j^2} & \text{for } u_i \neq u_j. \end{cases} \quad (13)$$

sans serif fonts are reserved here for components rewritten in a special vector basis composed of the stretch eigenvectors cf. (13). For the Hencky and Green strain measures this function reads, respectively

$$\widehat{\mathcal{A}}_{ijij} = \begin{cases} 1 & \text{for } i = j, \\ \frac{1}{2} & \text{for } \widehat{\boldsymbol{\varepsilon}}_i = \widehat{\boldsymbol{\varepsilon}}_j \text{ and } i \neq j, \\ \frac{\widehat{\boldsymbol{\varepsilon}}_i - \widehat{\boldsymbol{\varepsilon}}_j}{2 \sinh(\widehat{\boldsymbol{\varepsilon}}_i - \widehat{\boldsymbol{\varepsilon}}_j)} & \text{for } \widehat{\boldsymbol{\varepsilon}}_i \neq \widehat{\boldsymbol{\varepsilon}}_j, \end{cases} \quad \widehat{\mathcal{A}}_{ijij} = \begin{cases} u_i^2 & \text{for } i = j, \\ \frac{1}{2} u_i u_j & \text{for } i \neq j. \end{cases} \quad (14)$$

In Voigt notation the symmetric stress and strain tensors are treated as six-dimensional vectors in which the shear strain components take double values. Alternatively, in the Mandel notation the shear components both of the 6-dimensional stress and strain vectors are multiplied equally by $\sqrt{2}$. It is worth mentioning that representations of symmetric second-order tensors satisfy all postulates of the Euclidean six dimensional space. Thus, the two notations mentioned above are identified here with two representations of 6 dimensional vectors in two mutually different vector bases of a 6D Euclidean space, respectively. In order to distinguish components of vectors and tensors decomposed in $\mathbb{E}^3 \otimes \mathbb{E}^3$ and \mathbb{E}^6 , the elements of vector bases in \mathbb{E}^6 will be denoted here by Gothic characters, e.g. $\boldsymbol{\varepsilon}_{\mathfrak{x}}$ vs $\boldsymbol{\varepsilon}_a$ and $\boldsymbol{\varepsilon}_e$.

In the case of an orthonormal coordinate system in E^3 the scalar product of the stress and strain tensors used to determine the strain energy can be rewritten in the following form

$$\boldsymbol{\sigma} : \boldsymbol{\varepsilon} = \sigma_{11}\varepsilon_{11} + \sigma_{22}\varepsilon_{22} + \sigma_{33}\varepsilon_{33} + 2\sigma_{23}\varepsilon_{23} + 2\sigma_{31}\varepsilon_{31} + 2\sigma_{12}\varepsilon_{12}. \quad (15)$$

Representations of the tensors in Voigt notation will be identified here with the covariant and contravariant components of the following six-dimensional vectors

$$[\boldsymbol{\varepsilon}^{ij}]^T = [\varepsilon^1, \varepsilon^2, \varepsilon^3, \varepsilon^4, \varepsilon^5, \varepsilon^6]^T \equiv [\varepsilon_{11}, \varepsilon_{22}, \varepsilon_{33}, 2\varepsilon_{23}, 2\varepsilon_{13}, 2\varepsilon_{21}]^T, \quad (16a)$$

$$[\boldsymbol{\sigma}_{ij}] = [\sigma_1, \sigma_2, \sigma_3, \sigma_4, \sigma_5, \sigma_6] \equiv [\sigma_{11}, \sigma_{22}, \sigma_{33}, \sigma_{23}, \sigma_{13}, \sigma_{21}]. \quad (16b)$$

In such a case, the right hand of (15) can be treated as a scalar product of vector components rewritten in the Voigt vector basis for which the co- and contravariant representations of the unit tensor read

$$[\mathbf{g}_{ij\alpha\beta}] = \begin{bmatrix} 1 & \cdot & \cdot & \cdot & \cdot & \cdot \\ \cdot & 1 & \cdot & \cdot & \cdot & \cdot \\ \cdot & \cdot & 1 & \cdot & \cdot & \cdot \\ \cdot & \cdot & \cdot & \frac{1}{2} & \cdot & \cdot \\ \cdot & \cdot & \cdot & \cdot & \frac{1}{2} & \cdot \\ \cdot & \cdot & \cdot & \cdot & \cdot & \frac{1}{2} \end{bmatrix}, \quad [\mathbf{g}^{ij\alpha\beta}] = \begin{bmatrix} 1 & \cdot & \cdot & \cdot & \cdot & \cdot \\ \cdot & 1 & \cdot & \cdot & \cdot & \cdot \\ \cdot & \cdot & 1 & \cdot & \cdot & \cdot \\ \cdot & \cdot & \cdot & 2 & \cdot & \cdot \\ \cdot & \cdot & \cdot & \cdot & 2 & \cdot \\ \cdot & \cdot & \cdot & \cdot & \cdot & 2 \end{bmatrix}, \quad (17)$$

where ij denotes the Voigt type index corresponding to a pair of subscripts (i, j) used for tensors in $E^3 \otimes E^3$. In our notation, the pair of indices and its six dimensional counterpart in E^6 will be denoted by analogical symbols, e.g. ii and $\alpha\beta$ will be replaced their ligatures \ddot{i} , α , or simply by diacritical symbols obtained by overlapping the original ones, \ddot{i} and α . By analogy to classical force and displacement components, the components σ_{ij} and ε_{ij} will be identified here respectively with co- and contravariant representations of six dimensional stress and strain vectors, $\boldsymbol{\sigma}_{\ddot{i}}$ and $\boldsymbol{\varepsilon}^{\ddot{j}}$, respectively. For example, the volume density of strain energy can be rewritten in the form

$$\psi_V = \frac{1}{2} \boldsymbol{\sigma} : \boldsymbol{\varepsilon} = \frac{1}{2} \boldsymbol{\sigma}_{\ddot{i}} \boldsymbol{\varepsilon}^{\ddot{j}} = \frac{1}{2} \sigma_{ij} \varepsilon^{ij}. \quad (18)$$

2.2 Derivatives of tensor-valued functions

In Voigt notation the contravariant, covariant and mixed representations of the first derivative of a tensor-valued function of a symmetric second-order tensor, $\mathbf{f}(\mathbf{U})$, can be rewritten in the following form

$$\frac{\partial f^{\ddot{i}\ddot{j}}}{\partial U_{\ddot{k}}} = \begin{cases} f'(\lambda_i) & \text{for } i = j, \\ 2f'(\lambda_i) & \text{for } \begin{cases} \lambda_i = \lambda_j \\ i \neq j, \end{cases} \\ 2\frac{f(\lambda_i) - f(\lambda_j)}{\lambda_i - \lambda_j} & \text{for } \lambda_i \neq \lambda_j, \end{cases} \quad (19)$$

$$\frac{\partial f_{\ddot{i}\ddot{j}}}{\partial U^{\ddot{k}}} = \begin{cases} f'(\lambda_i) & \text{for } i = j, \\ \frac{1}{2}f'(\lambda_i) & \text{for } \begin{cases} \lambda_i = \lambda_j \\ i \neq j, \end{cases} \\ \frac{1}{2}\frac{f(\lambda_i) - f(\lambda_j)}{\lambda_i - \lambda_j} & \text{for } \lambda_i \neq \lambda_j. \end{cases} \quad (20)$$

$$\frac{\partial f^{\ddot{i}\ddot{j}}}{\partial U^{\ddot{k}}} = \frac{\partial f_{\ddot{i}\ddot{j}}}{\partial U_{\ddot{k}}} = \begin{cases} f'(\lambda_i) & \text{for } \lambda_i = \lambda_j, \\ \frac{f(\lambda_i) - f(\lambda_j)}{\lambda_i - \lambda_j} & \text{for } \lambda_i \neq \lambda_j, \end{cases} \quad (21)$$

The mentioned representations satisfy the following transformation rule $\frac{\partial f^{\alpha\beta}}{\partial U^{\gamma\delta}} = \mathbf{g}^{\alpha\beta\gamma\delta} \frac{\partial f_{\mu\nu}}{\partial U^{\mu\nu}} = \mathbf{g}^{\alpha\beta\gamma\delta} \frac{\partial f_{\mu\nu}}{\partial U^{\mu\nu}} \mathbf{g}^{\mu\nu\kappa\lambda} = \mathbf{g}^{\alpha\beta\gamma\delta} \frac{\partial f^{\mu\nu}}{\partial U^{\mu\nu}} \mathbf{g}_{\mu\nu\kappa\lambda}$.

A 6x6 dimensional unit tensor \mathbf{g} can be spanned on two different vector bases. Then, the shifters $\mathbf{g}^{\alpha\beta\gamma\delta}$ give possibility to transform the tensor components from one vector basis to another, e.g. from the Voigt vector basis to the orthonormal one in E^6 .

Analytic formulas for $\frac{\partial \mathbf{f}^2}{\partial \mathbf{U}}$ take a more complex form than those for $\frac{\partial \mathbf{f}}{\partial \mathbf{U}}$. The first derivation of such analytic formulas (not quite correct) is due to Bowen and Wang [2], see (3.50-3.61) therein. In 1971 Chadwick and Ogden presented the results of an independent calculation in which the main errors of Bowen and Wang [2] were corrected.

As a matter of fact, they repeated some errors after Bowen and Wang. In result, it seems that in none of papers published as of yet the mentioned equations have been corrected. In 2008, Norris [43] presented in a smart form a general mathematical scheme for calculation of an n^{th} -order derivative, see (3.16) therein. The present authors, not being quite convinced which form of the formulas for the second derivative is correct, have performed a series of the validation tests. Due to the non-orthonormality of the Voigt vector basis $\{\mathbf{e}_{\mathbf{x}}\}$, the first test was performed for the mixed representation by means of the standard finite difference scheme adopted here to E^6 ,

$$\frac{\partial^2 f_{ij}}{\partial U_{\mathbf{x}} \partial U_{\mathbf{x}}} = \frac{f_{ij}(\mathbf{U} + \Delta_{\mathbf{x}}) - 2f_{ij}(\mathbf{U}) + f_{ij}(\mathbf{U} - \Delta_{\mathbf{x}})}{\Delta_{\mathbf{x}} \Delta_{\mathbf{x}}}, \quad (22a)$$

$$\frac{\partial^2 f_{ij}}{\partial U_{\mathbf{x}} \partial U_{fl}} = \frac{f_{ij}(\mathbf{U} + \Delta_{\mathbf{x}} + \Delta_{fl}) - f_{ij}(\mathbf{U} - \Delta_{\mathbf{x}} + \Delta_{fl}) - f_{ij}(\mathbf{U} + \Delta_{\mathbf{x}} - \Delta_{fl}) + f_{ij}(\mathbf{U} - \Delta_{\mathbf{x}} - \Delta_{fl})}{4 \Delta_{\mathbf{x}} \Delta_{fl}} \quad (22b)$$

where $[\Delta_{\mathbf{x}}]^T = [U_1, \dots, U_{\mathbf{x}} + \Delta_{\mathbf{x}}, \dots, U_6]^T$. After this test had passed, the following correct contravariant representation (23) was fixed by using the chain rule $\frac{\partial^2 f^{ii}}{\partial U^{\mathbf{x}} \partial U^{\mathbf{fl}}} = \mathfrak{g}^{ii} \frac{\partial^2 f_{ij}}{\partial U^{\mathbf{x}} \partial U^{\mathbf{fl}}}$,

$$\frac{\partial^2 f^{ij}}{\partial U_{\mathbf{j}} \partial U_{\mathbf{ki}}} = \begin{cases} f''(\lambda_i) & \text{for } \lambda_i = \lambda_j = \lambda_k, \\ 2 \frac{f'(\lambda_j) - \frac{f(\lambda_i) - f(\lambda_j)}{\lambda_i - \lambda_j}}{(\lambda_i - \lambda_j)} & \text{for } \lambda_i \neq \lambda_j = \lambda_k, \\ -2 \frac{f(\lambda_i)(\lambda_j - \lambda_k) + f(\lambda_j)(\lambda_k - \lambda_i) + f(\lambda_k)(\lambda_i - \lambda_j)}{(\lambda_i - \lambda_j)(\lambda_j - \lambda_k)(\lambda_k - \lambda_i)} & \text{for } \lambda_i \neq \lambda_j \neq \lambda_k \neq \lambda_i, \end{cases} \quad (23)$$

where the subscripts i, j, k run over all possible values: 1, 2, 3. In order to compare our results with those presented in the previous papers it is convenient to rewrite $\mathcal{L}_{ijklmn}^{(2)} = \frac{\partial^2 f_{ij}}{\partial U^{kl} \partial U^{mn}}$ in the following form

$$\mathcal{L}_{iiii}^{(2)} = f''(\lambda_i), \quad (24a)$$

$$\mathcal{L}_{iiij}^{(2)} = \begin{cases} \frac{1}{4} f''(\lambda_i) & \text{for } \lambda_i = \lambda_j, \\ \frac{1}{2} \frac{\frac{f(\lambda_i) - f(\lambda_j)}{\lambda_i - \lambda_j} - f'(\lambda_i)}{(\lambda_i - \lambda_j)} & \text{for } \lambda_i \neq \lambda_j, \end{cases} \quad (24b)$$

$$\mathcal{L}_{ijjki}^{(2)} = \begin{cases} \frac{1}{8} f''(\lambda_i) & \text{for } \lambda_i = \lambda_j = \lambda_k, \\ \frac{1}{4} \frac{\frac{f(\lambda_i) - f(\lambda_j)}{\lambda_j - \lambda_i} - f'(\lambda_j)}{(\lambda_j - \lambda_i)} & \text{for } \lambda_i \neq \lambda_j = \lambda_k, \\ -\frac{1}{4} \frac{f(\lambda_i)(\lambda_j - \lambda_k) + f(\lambda_j)(\lambda_k - \lambda_i) + f(\lambda_k)(\lambda_i - \lambda_j)}{(\lambda_i - \lambda_j)(\lambda_j - \lambda_k)(\lambda_k - \lambda_i)} & \text{for } \lambda_i \neq \lambda_j \neq \lambda_k \neq \lambda_i, \end{cases} \quad (24c)$$

where only $i \neq j \neq k$ take possible values: 1, 2, 3. The terms corrected here have been rewritten in bold, cf. (3.5.33–34) in [44]. The question then arises how it was possible that so many years a formula so important for calculation of the second derivatives of a tensor-valued functions have not been corrected. Recently, most of the complex analytic differentiation is computed by means of programs for symbolic calculations. Such programs are very useful under one condition, namely, that somebody earlier has programmed a given analytic operation. Otherwise, there is rather a small chance that a given error will be detected by means of elemental operations already programmed in.

3 Anisotropic hyperelasticity and TOECs in terms of logarithmic strain

In the case of quasistatic elastic deformation of an anisotropic body, the local form of the energy balance law can be rewritten in the following way

$$-\rho \dot{\psi} + \boldsymbol{\sigma} : \mathbf{d} = 0, \quad (25)$$

where ρ , $\dot{\psi}$ and $\boldsymbol{\sigma}$ respectively denote the mass density, material derivative of strain energy, and the Cauchy stress. Suppose that the specific strain energy depends on the Lagrangian strain tensor

$$\psi = \psi(\hat{\boldsymbol{\varepsilon}}). \quad (26)$$

Substitution of (26) and (12) into (25) gives

$$-\frac{\rho}{\hat{\rho}} \left(\hat{\rho} \frac{\partial \psi}{\partial \hat{\boldsymbol{\varepsilon}}} \right) : \hat{\boldsymbol{\mathcal{A}}} : (\mathbf{R}^T \mathbf{d} \mathbf{R}) + \boldsymbol{\sigma} : \mathbf{d} = 0, \quad (27)$$

Eulerian configuration		Lagrangian configuration	
Name	Formula	Name	Formula
Hencky	$\ln \mathbf{V}$	Hencky	$\ln \mathbf{U}$
Swainger	$\mathbf{1} - \mathbf{V}^{-1}$	Biot	$\mathbf{U} - \mathbf{1}$
Alamansi	$\frac{1}{2}(\mathbf{1} - \mathbf{V}^{-2})$	Green	$\frac{1}{2}(\mathbf{U}^2 - \mathbf{1})$

Table 1: Eulerian and Lagrangian strains conjugate by the transformation tensor \mathcal{A} , cf. (32b).

where $\hat{\rho} = \rho \det \mathbf{F}$. To balance the energy for an arbitrarily chosen \mathbf{d} , the Cauchy stress has to be governed by the following transformation rule

$$\boldsymbol{\sigma} = \mathbf{R}(\hat{\mathcal{A}} : \hat{\boldsymbol{\sigma}})\mathbf{R}^T \det \mathbf{F}^{-1}, \quad (28)$$

where the stress conjugate to the given Lagrangian strain reads

$$\hat{\boldsymbol{\sigma}} \stackrel{df}{=} \hat{\rho} \frac{\partial \psi}{\partial \hat{\boldsymbol{\varepsilon}}}. \quad (29)$$

Constitutive equations for anisotropic Hookean model can be derived by assuming the following strain energy function

$$\hat{\rho} \psi(\hat{\boldsymbol{\varepsilon}}) = \frac{1}{2} \hat{\boldsymbol{\varepsilon}} : \hat{\mathbf{c}} : \hat{\boldsymbol{\varepsilon}}, \quad (30)$$

where, by definition, $\hat{\mathbf{c}} = \text{const}$. The substitution subsequently into (29) and (28) gives

$$\hat{\boldsymbol{\sigma}} = \hat{\mathbf{c}} : \hat{\boldsymbol{\varepsilon}} \quad \text{and} \quad \boldsymbol{\sigma} = \mathbf{c} : \boldsymbol{\varepsilon}, \quad (31)$$

where the Eulerian strain and stiffness tensors are defined by means of the following transformation rules

$$\boldsymbol{\varepsilon} \stackrel{df}{=} \mathcal{A}^{-1} : \hat{\boldsymbol{\varepsilon}}, \quad \mathbf{c} \stackrel{df}{=} \mathcal{A}^T : \hat{\mathbf{c}} : \mathcal{A} \det \mathbf{F}^{-1}, \quad (32)$$

where $\mathcal{A}_{IJ}^{ij} \stackrel{df}{=} R^i_K R^j_L \hat{\mathcal{A}}^{KL}$ and $\mathcal{A}^{-1}_{ij}{}^{IJ} = R_i^K R_j^L \hat{\mathcal{A}}^{-1}{}^{IJ}{}_{KL}$. According to this transformation rule, Almansi strain in the Eulerian configuration is obtained as the Eulerian counterpart of Green strain, cf. Table 1. In the literature, different notations and names are used. In the present paper, the tensors called the Eulerian and Lagrangian Almansi strains differ each other only the rigid rotation.

Assume further that a hyperelastic material satisfies the following strain energy function

$$\psi(\hat{\boldsymbol{\varepsilon}}) = \frac{1}{\hat{\rho}} \left[\frac{1}{2!} \hat{\mathbf{c}}_{ijkl} \hat{\boldsymbol{\varepsilon}}^{ij} \hat{\boldsymbol{\varepsilon}}^{kl} + \frac{1}{3!} \hat{\mathbf{C}}_{ijklm} \hat{\boldsymbol{\varepsilon}}^{ij} \hat{\boldsymbol{\varepsilon}}^{kl} \hat{\boldsymbol{\varepsilon}}^{lm} \right], \quad (33)$$

where $\hat{\mathbf{c}}$ and $\hat{\mathbf{C}}$ are tensors of the second and third-order elastic coefficients determined in relation to a given strain measure. Substitution of (33) into (29) gives the following equation for the conjugate stress

$$\hat{\boldsymbol{\sigma}} = \hat{\mathbf{c}} : \hat{\boldsymbol{\varepsilon}} + \frac{1}{2} \hat{\boldsymbol{\varepsilon}} : \hat{\mathbf{C}} : \hat{\boldsymbol{\varepsilon}}. \quad (34)$$

Each of strain measures from the Seth-Hill family can be recalculated to another one from the same family by means of the following transformation rule

$$\hat{\boldsymbol{\varepsilon}}'(\hat{\boldsymbol{\varepsilon}}) = \begin{cases} \frac{1}{m'} [(m\hat{\boldsymbol{\varepsilon}} + \mathbf{1})^{\frac{m'}{m}} - \mathbf{1}] & \text{for } m \neq 0 \wedge m' \neq 0, \\ \frac{1}{m'} [\exp(m'\hat{\boldsymbol{\varepsilon}}) - \mathbf{1}] & \text{for } m = 0 \wedge m' \neq 0, \\ \frac{1}{m} \ln(m\hat{\boldsymbol{\varepsilon}} + \mathbf{1}) & \text{for } m \neq 0 \wedge m' = 0. \end{cases} \quad (35)$$

It is easy to shown that SOECs are invariant with respect to the choice of strain measure. Contrary to that, TOECs depend very strongly on the choice of strain measure. In other words, two experimenters observing the same run of instantaneous stiffness under loading can determine two dramatically different sets of TOECs. Thus, in order to refer to the same initial 2nd order instantaneous stiffness by constitutive models based on different strain measures, TOECs must be recalculated from the strain for which TOECs had been determined experimentally to the strain measure

$\hat{\varepsilon} = \frac{1}{m}(\mathbf{U}^m - \mathbf{1})$	\hat{C}_{111}	\hat{C}_{112}	\hat{C}_{123}	\hat{C}_{144}	\hat{C}_{155}	\hat{C}_{456}	$\partial\hat{B}/\partial\hat{\varepsilon}$	m
Green	-815	-450	-75	16	-307	-82	-1124	2
Biot	-317	-386	-75	48	-170	-22	-928	1
Hencky	181	-322	-75	80	-32	38	-544	0
Almansi	1177	-194	-75	144	243	158	-46	-2
	1254	-184	-75	149	266	167	0	-2.155

Table 2: Silicon crystal third-order elastic coefficients [GPa] related to different strain measures.

which is used in a given constitutive model. The formulas for recalculation of TOECs have been given by Dłuzewski [13],

$$\hat{C}'_{ijklm} = \hat{C}_{ijklm} + (m - m') [\mathcal{J}_{ijkl}^{\otimes} \hat{c}_{\otimes mm} + \mathcal{J}_{klm}^{\otimes} \hat{c}_{\otimes ij} + \mathcal{J}_{mij}^{\otimes} \hat{c}_{\otimes kl}], \quad (36)$$

where \mathcal{J} is a sixth-order proper-symmetric unit tensor.

Apply (36) to recalculation of TOECs. According to the method proposed by Thurston et al. [52], the 2-nd order instantaneous stiffness change of silicon crystal had been measured by Johal and Dunstan [29] and stored in the form of TOECs related to Green strain measure, see Table 2. SOECs obtained by them were $\hat{c}_{11} = 166$ GPa, $\hat{c}_{12} = 64$ GPa, $\hat{c}_{44} = 80$ GPa. In the case of cubic crystal, (36) reads [13]

$$\begin{aligned} \hat{C}'_{111} &= \hat{C}_{111} + 3(m - m') \hat{c}_{11}, & \hat{C}'_{144} &= \hat{C}_{144} + \frac{1}{2}(m - m') \hat{c}_{12}, \\ \hat{C}'_{112} &= \hat{C}_{112} + (m - m') \hat{c}_{12}, & \hat{C}'_{155} &= \hat{C}_{155} + (m - m') \left[\hat{c}_{44} + \frac{1}{4} \hat{c}_{12} + \frac{1}{4} \hat{c}_{11} \right], \\ \hat{C}'_{123} &= \hat{C}_{123}, & \hat{C}'_{456} &= \hat{C}_{456} + \frac{3}{4}(m - m') \hat{c}_{44}. \end{aligned} \quad (37)$$

Thus, TOECs have been recalculated here onto equivalent TOECs referred to a few mutually different strain measures, see rows 3,4 and 5 in Table 2. Additionally, in the last row the strain measure has been chosen in such a way to get a Hookean for which the second-order bulk modulus vanishes. Namely, the substitution of $\hat{\mathbf{c}} = \hat{\mathbf{c}}^\circ + \hat{\mathbf{C}} : \hat{\varepsilon}$ into $\hat{B} = \frac{\hat{c}_{11} + 2\hat{c}_{12}}{3}$ gives the following dependence of bulk modulus on the volume strain $\hat{\varepsilon}$

$$\hat{B}(\hat{\varepsilon}) = \frac{\hat{c}_{11}^\circ + 2\hat{c}_{12}^\circ}{3} + \frac{\hat{C}_{111} + 6\hat{C}_{112} + 2\hat{C}_{123}}{3} \hat{\varepsilon} \quad (38)$$

where $\hat{\varepsilon} = \hat{\varepsilon}^1 = \hat{\varepsilon}^2 = \hat{\varepsilon}^3$. One can check that $\frac{dB}{d\hat{\varepsilon}}$ vanishes for $m' = m + \frac{\hat{C}_{111} + 6\hat{C}_{112} + 2\hat{C}_{123}}{3\hat{c}_{11} + 6\hat{c}_{12}}$.

3.1 Uniaxial stretch test

In this case the axial component of Hencky strain changes proportionally to the relative change of the length of sample, according to the differential form

$$d\hat{\varepsilon} = d(\ln U) = \frac{dl}{l}. \quad (39)$$

Bearing in mind (39), it is easy to note that

$$\lim_{\Delta l \rightarrow 0} \frac{\Delta \sigma_{11}}{\frac{\Delta l}{l}} = \frac{d\sigma_{11}}{d(\ln F_{11})} = \frac{d\sigma_{11}}{dF_{11}} \frac{dF_{11}}{d(\ln F_{11})} = \frac{d\sigma_{11}}{dF_{11}} F_{11}. \quad (40)$$

This means that the increase of Hencky strain is invariant with respect to the choice of the reference configuration. For this reason, Hencky strain was initially regarded as a measure for which Hooke's law holds a constant instantaneous stiffness. Nevertheless, the strain energy is referred to the mass density thus, also the instantaneous stiffness changes during the uniaxial deformation process. The Hookean extended by TOECs term leads to the following relationship for the Cauchy stress

$$\sigma = \begin{cases} c_\circ F^{m-1} \frac{1}{m} (F^m - 1) + \frac{1}{2} C_\circ F^{m-1} \frac{1}{m^2} (F^m - 1)^2 & \text{for } m \neq 0, \\ c_\circ F^{-1} \ln F + \frac{1}{2} C_\circ F^{-1} \ln^2 F & \text{for } m = 0, \end{cases} \quad (41)$$

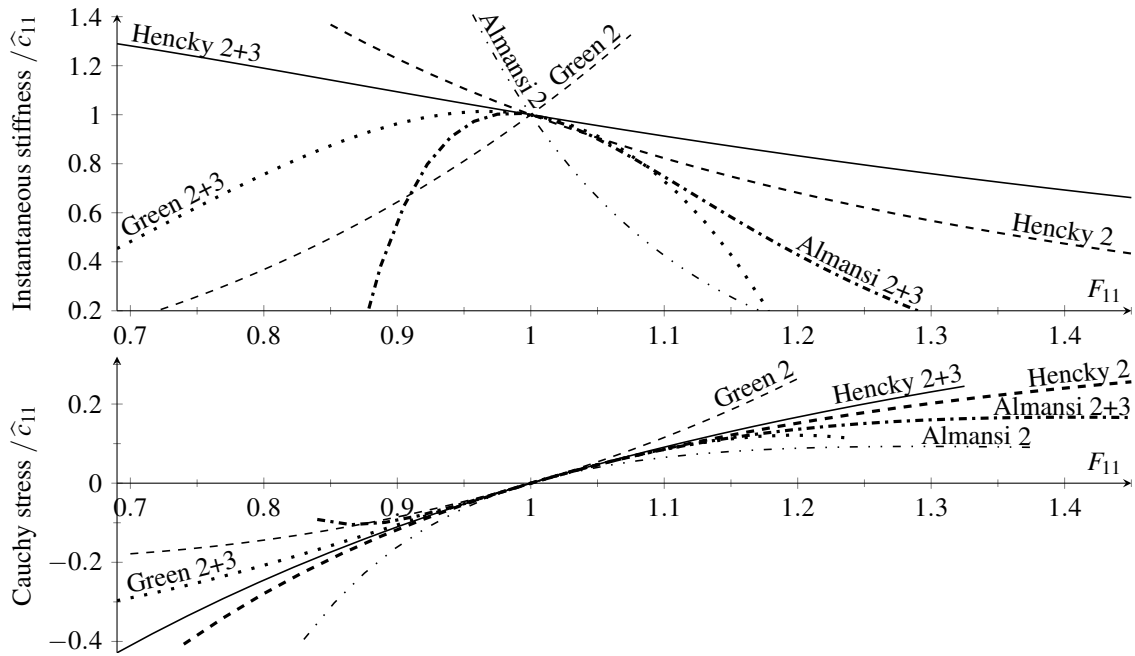


Figure 1: Instantaneous stiffness and Cauchy stress curves for constitutive models obtained by adding third-order elastic terms to Hookean models in uniaxial stretch test, *cf.* Table 2.

where $\sigma = \sigma_{11}$, $F = F_{11}$, $c_o = \hat{c}_{1111}$ and $C_o = \hat{C}_{111111}$. In order to hold the same 2nd order instantaneous stiffness in the relaxed configuration by different constitutive models, the TOECs must be recalculated first to the values corresponding to strain measure used in the given constitutive model. From a mathematical point of view, the instantaneous stiffness tensor is identified with the derivative of Cauchy stress over the deformation gradient in the current configuration assumed to be the reference one, see [44]. As an example, consider the behaviour of the 2nd and 3rd order hyperelastic models of silicon crystal. In contrast to SOECs, the TOECs have been recalculated according to the state-of-the-art discussed above, see (36) and Table 1. Thanks to such a chosen transformation rule, all of the third-order elastic models hold the same, experimentally observed change of *instantaneous* stiffness in the vicinity of the relaxed configuration. In other words, despite of the different TOECs used, the Cauchy stress and instantaneous stiffness diagrams shown in Fig. 1 for Green 2+3, Hencky 2+3, Almansi 2+3, have the same initial slope corresponding to the experimentally observed instantaneous stiffness evolution, *cf.* $\left. \frac{d^2 \sigma}{dF_{11}^2} \right|_{F_{11}=1}$. All runs shown have been normalized by dividing both the axial Cauchy stress and instantaneous stiffness by \hat{c}_{111} .

It is worth emphasizing that a one-dimensional Hookean model of atomic bond based on the use of Hencky strain demonstrates the constant stiffness of atomic bond. As is shown in solid physics the stiffness of atomic bonds decrease together with stretching the bonds. Obviously, these two effects, the volume change vs the change of single atomic bonds stiffness, having two mutually different origin, contribute together in the overall response of elastic material as a whole. It was shown in many papers that Hookean based on Hencky strain pretty well approximates the atomistic simulations for many monocrystals, see e.g. [14, 37].

4 TOECs in finite element modelling

In many iterative schemes applied in solving nonlinear FE problems the important role takes the correct determination of the tangent stiffness matrix. In order to limit considerations to matrix components resulting from constitutive equations discussed above, we consider the classical quasi-static problem. In such a case, the total potential energy Π is defined as

$$\Pi = \int_V \hat{\rho} \psi \det \mathbf{F}^{-1} dv - \Pi_{\text{ext}}, \quad (42)$$

where $\Pi_{\text{ext}} = \int_{\partial V} \mathbf{u} \sigma ds$ denotes the potential of external traction forces acting on the surface ∂V bounding the volume region V . In the case of the isoparametric finite elements, the virtual displacement field is determined by the following

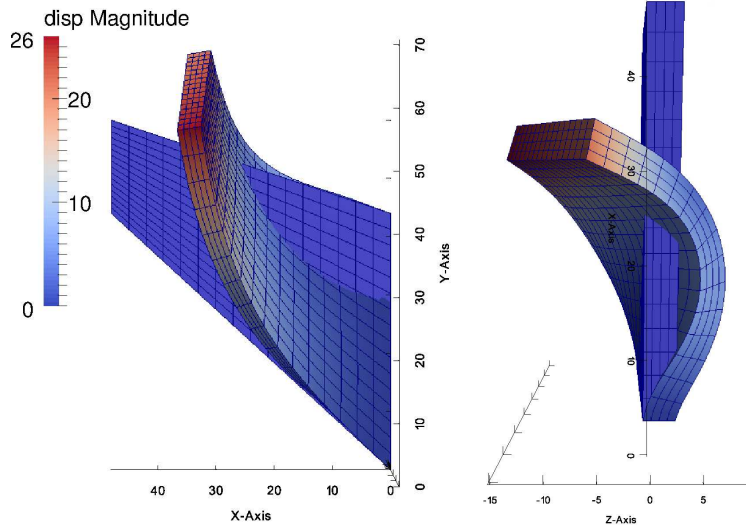


Figure 2: Cook's membrane problem. The initial and final configurations for the Hencky 2+3 model and Si nanomembrane orientation [075](357).

relation: $\delta u^i = \sum_m N_{mi} \delta a_m^i$, where N_{mi} and δa_m^i denote the shape function and a variation of i -th displacement component at node m , respectively. For isoparametric elements, the same shape function is assumed for all spatial position vectors and displacement vectors, i.e. $N_{m1}(\mathbf{a}_1, \dots, \mathbf{a}_n) = N_{m2}(\mathbf{a}_1, \dots, \mathbf{a}_n) = N_{m3}(\mathbf{a}_1, \dots, \mathbf{a}_n) = N_m(\mathbf{a}_1, \dots, \mathbf{a}_n)$. Nevertheless, to distinguish which shape function and gradients relate to which nodal displacement component, we save in our notation the displacement component index and write it in serif letters contrary to italics denoting the co- and contravariant components of vectors and tensors, respectively. The variation of total energy (42) can be rewritten as

$$\delta \Pi = \delta a_m^i \int_V \hat{\rho} \frac{\partial \Psi}{\partial \hat{\epsilon}_{IJ}} \frac{\partial \hat{\epsilon}_{IJ}}{\partial a_m^i} \det \mathbf{F}^{-1} dv - \delta a_m^i \int_{\partial V} N_{mi} \sigma_{ij} n^j ds. \quad (43)$$

where

$$\frac{\partial \hat{\epsilon}_{KL}}{\partial a_m^i} = \frac{1}{2} \mathcal{A}_{KL}{}^{kl} (g_{ik} N_{mi,l} + g_{il} N_{mi,k}). \quad (44)$$

Thus, the elimination of virtual displacements from (43) leads to the following nonlinear equation

$$P_{mi} \stackrel{df}{=} \frac{1}{2} \int_V (g_{ik} N_{mi,l} + g_{il} N_{mi,k}) \sigma^{kl} dv - \int_{\partial V} N_{mi} \sigma_{ij} n^j ds = 0. \quad (45)$$

where P_{mi} is the i -th component of the residual vector in the m -th node. As shown in Appendix, such obtained tangent stiffness matrix takes form

$$K_m^i n^j = \int_V N_{mi,k} \left[\left(\mathcal{A}_{PR}{}^{ik} \frac{\partial \hat{\sigma}^{PR}}{\partial \hat{\epsilon}_{ST}} \mathcal{A}_{ST}{}^{jl} + \mathcal{B}_{PR}{}^{ikjl} \hat{\sigma}^{PR} \right) \det \mathbf{F}^{-1} + g^{ij} \sigma^{kl} \right] N_{nj,l} dv. \quad (46)$$

4.1 Numerical example

As a FE test we consider a three dimensional variant of the Cook's membrane made of 4 nm thick silicon crystal, see Fig.2. The problem is analysed with and without the use of TOECs related to the Hencky and Green strain measures, respectively; see Table 2. The membrane is discretized into $16 \times 16 \times 4$ isoparametric Lagrange brick elements with quadratic interpolation [36]. The shape and boundary conditions are assumed here in the similar way to those considered among others by Menzel and Steinmann [39]. The front vertical wall of membrane is conservatively loaded by a uniformly distributed vertical traction force corresponding 3.75 GPa. We consider two lattice orientations of the nanomembrane, [001](100) and [075](357), where the Miller indices in the round and square brackets denote respectively the crystal orientation of nanomembrane plane and the lattice vector direction x on that plane.

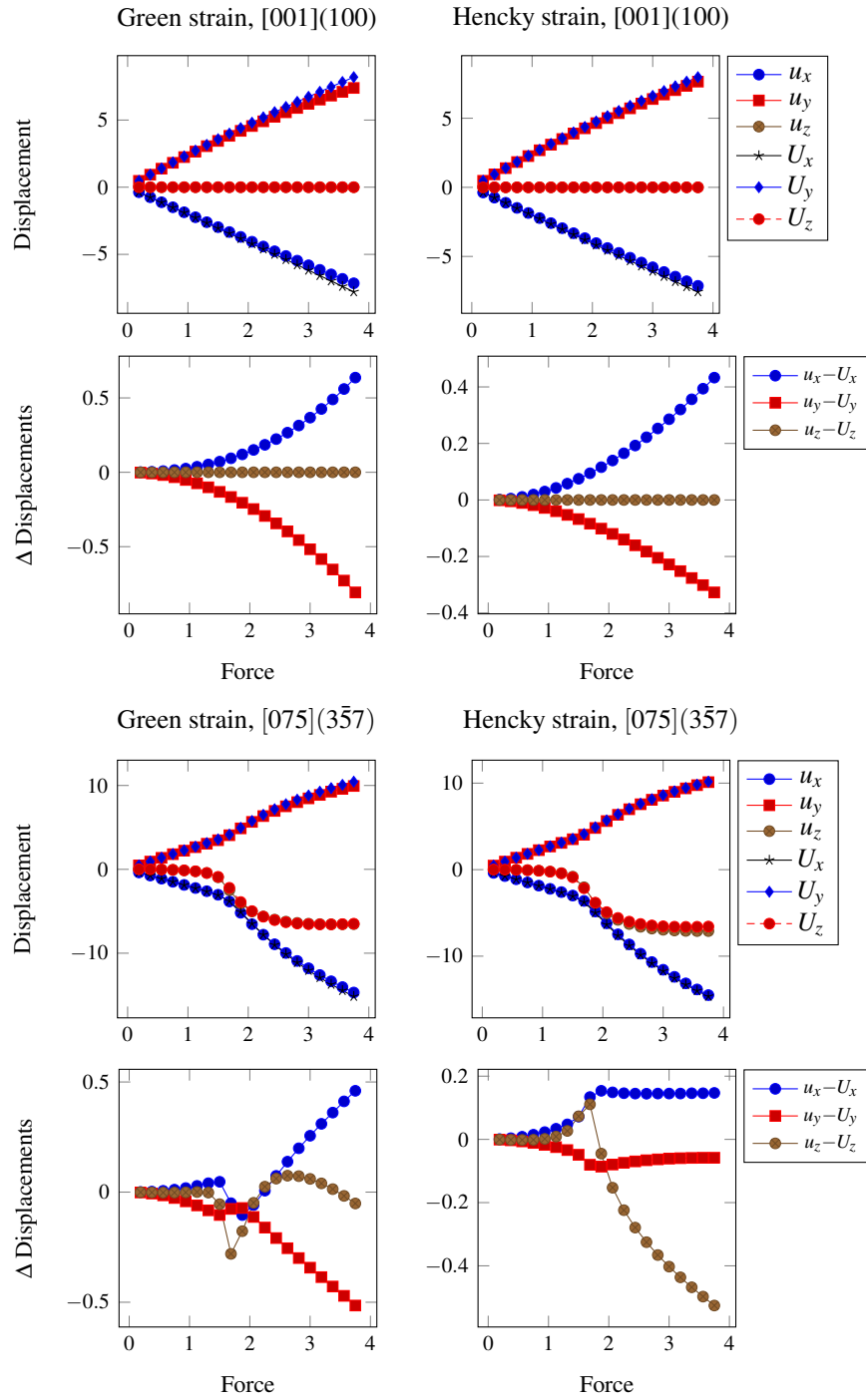


Figure 3: (Top) Displacements u_x, u_y, u_z and U_x, U_y, U_z obtained without and with use of the 3rd order elastic coefficients for different strain measures and different lattice orientations. (Bottom) Difference between the displacements of nanomembrane.

The resultant displacements of the mid point of the top edge of the nanomembrane are presented in Fig. 3. For symmetric crystal lattice orientation $[001](100)$ the difference in displacements yielding from the use of TOECs does not exceed 10%, see Fig. 3. For asymmetric lattice orientation $[075](3\bar{5}7)$, the nanomembrane bucked both for the use of the Green as well as Hencky strain measures. The use of different lattice orientation significantly changed the behaviour of the nanomembrane, while the adding of TOECs changed its displacements up to 10%. In Fig. 2, the views xy and xz of the initial and deformed mesh for the $[075](3\bar{5}7)$ lattice orientation and the use of TOECs related to Hencky strain is shown.

5 Conclusions

In acoustic measurements, according to tradition, TOECs are determined in relation to the Green strain [28, 51]. On the other hand, in ab-initio calculations, TOECs are often determined with the use of Biot strain measure, e.g. $\epsilon_{11} = \frac{a-a_0}{a_0}$. In result, the coefficients obtained by means of these two methods can differ from each other dramatically. As shown in Table 2 the coefficient $C_{111} = -317$ GPa determined experimentally with the use of Green strain is equivalent to $C_{111} = -815$ GPa determined with the use of Biot strain. This is because each Hookean hardens in a different way, see Fig. 1. As a matter of fact, TOECs are nothing more than the correction chosen for a given Hookean towards the experimentally fixed stress-stretch curve. In order to use TOECs with another strain measure than that of used in experimental measurement, the coefficients must be recalculated first to the given strain measure, see formula (36) and (37) derived by Dłużewski in [13]. It is worth emphasizing that the replacement of Green strain by Hencky strain leads generally to the decreasing of TOECs, cf. Table 2.

The convergence of iterative schemes applied in solving of FE boundary-value problems often depends strongly on the correct calculation of the stiffness matrix. In this paper the analytic formulas for the tangent stiffness calculation for Hookeans based on general Lagrangian strain have been corrected. The use of Hencky strain in FE calculations is not a new problem, and many validation tests comparing the convergence of different algorithms were done in the past [19, 39, 40]. Due to the corrections presented here, an open question arises as to how far these errors burdened results of such validation tests in the past, cf. the use of (24b) and their counterparts in the concurrent numerical schemes. From the viewpoint of our computational practice, errors of this kind can limit the convergence region and/or increase the computing time especially for the problems with expected symmetries in the resulting stress/strain fields.

Acknowledgement

This research was supported by the Polish Ministry of Science and Higher Education grant NN519 647640.

References

- [1] F. Birch. Finite elastic strain of cubic crystals. *Physical Review*, 71:809–824, Jun 1947. doi: 10.1103/PhysRev.71.809.
- [2] R.M. Bowen and C.-C. Wang. Acceleration waves in inhomogeneous isotropic elastic bodies. *Archive of Rational Mechanics and Analysis*, 38, 1970. doi: 10.1007/BF00251539. with Corrigendum in vol. 40, 403.
- [3] K. Brugger. Thermodynamic definition of higher order elastic coefficients. *Physical Review*, 133(6A):1611–12, 1964. doi: 10.1103/PhysRev.133.A1611.
- [4] M.M. Carroll. Must Elastic Materials be Hyperelastic? *Mathematics and Mechanics of Solids*, 14(4):369–376, 2009. doi: 10.1177/1081286508099385.
- [5] P. Chadwick and R.W. Ogden. A theorem of tensor calculus and its application to isotropic elasticity. *Archive for Rational Mechanics and Analysis*, 44(1):54–68, 1971. ISSN 0003-9527. doi: 10.1007/BF00250828.
- [6] T. Chipanga. *Determination of the Accuracy of Residual Stress Measurement Methods Hole Drilling, Ultrasonic (Debro-30) System and Digital Shearography*. Lambert Academic Publishing, 2010. URL <http://www.lap-publishing.com/>.
- [7] J. Cholewiński, M. Maździarz, G. Jurczak, and P. Dłużewski. Dislocation core reconstruction based on finite deformation approach and its application to 4H-SiC crystal. *International Journal for Multiscale Computational Engineering*, 12:411421, 2014. doi: 10.1615/IntJMultCompEng.2014010679.

- [8] J.D. Clayton. Analysis of shock compression of strong single crystals with logarithmic thermoelastic-plastic theory. *International Journal of Engineering Science*, 79(0):1 – 20, 2014. ISSN 0020-7225. doi: 10.1016/j.ijengsci.2014.02.016.
- [9] C. S. G. Cousins. Elasticity of carbon allotropes. I. Optimization, and subsequent modification, of an anharmonic Keating model for cubic diamond. *Physical Review B*, 67:024107, Jan 2003. doi: 10.1103/PhysRevB.67.024107.
- [10] Z. Curnier and Ph. Zysset. A family of metric strains and conjugate stresses, prolonging usual material laws from small to large transformations. *International Journal of Solids and Structures*, 43:3057–3086, 2006. doi: 10.1016/j.ijsolstr.2005.06.015.
- [11] J. Deputat, J. Szelazek, and M. Adamski. *Experiences in Ultrasonic Measurements of Stresses in Rails*, pages 109–118. Springer Netherlands, Dordrecht, 1993. ISBN 978-94-015-8151-6. doi: 10.1007/978-94-015-8151-6_9.
- [12] M. Destrade and R.W. Ogden. On the third- and fourth-order constants of incompressible isotropic elasticity. *Journal of the Acoustical Society of America*, 128(6):3334–3343, 2010. doi: 10.1121/1.3505102.
- [13] P. Dłużewski. Anisotropic hyperelasticity based upon general strain measures. *Journal of Elasticity*, 60(2): 119–129, 2000. doi: 10.1023/A:1010969000869.
- [14] P. Dłużewski and P. Traczykowski. Numerical simulation of atomic positions in quantum dot by means of molecular statics. *Archive of Mechanics*, 55:501–515, 2003.
- [15] D.M. Egle and D.E. Bray. Measurement of acoustoelastic and third-order elastic constants for rail steel. *J. Acoust. Soc. Am.*, 60:741, 1969. doi: 10.1121/1.381146.
- [16] B. Feng, V.I. Levitas, and R.J. Hemley. Large elastoplasticity under static megabar pressures: Formulation and application to compression of samples in diamond anvil cells. *International Journal of Plasticity*, 84:33 – 57, 2016. ISSN 0749-6419. doi: 10.1016/j.ijplas.2016.04.017.
- [17] M.D. Frogley, J.R. Downes, and D.J. Dunstan. Theory of the anomalously low band-gap pressure coefficients in strained-layer semiconductor alloys. *Physical Review B*, 62:13612–13616, Nov 2000. doi: 10.1103/PhysRevB.62.13612.
- [18] F.F. Gantmacher, *The theory of matrices*. Goz. Izdat. Lit., Moscow, 1954; English transl., Applications of the theory of matrices, Interscience, New York, 1959, 1954.
- [19] S. Germain, M. Scherer, and P. Steinmann. On inverse form finding for anisotropic hyperelasticity in logarithmic strain space. *International Journals of Structural Changes in Solids – Mechanics and Applications*, 2(2):1–16, 2010.
- [20] R.E. Hankey and D.E. Schuele. Third-order elastic constants of Al_2O_3 . *Journal of the Acoustical Society of America*, 48(1B):190–202, 1970. doi: 10.1121/1.1912116.
- [21] N.J. Higham. *Functions of Matrices: Theory and Computation*. Society for Industrial and Applied Mathematics, Philadelphia, PA, USA, 2008. ISBN 978-0-898716-46-7.
- [22] Y. Hiki and A.V. Granato. Anharmonicity in noble metals; higher order elastic constants. *Physical Review*, 144 (2):411–19, 1966. doi: 10.1103/PhysRev.144.411.
- [23] R. Hill. Constitutive inequalities for isotropic solids under finite strain. *Proceedings of Royal Society of London A*, 314:457–472, 1970. doi: 10.1098/rspa.1970.0018.
- [24] R. Hill. Aspects of invariance in solid mechanics. *Advances in Applied Mechanics*, 18:1–75, 1978. doi: 10.1016/S0065-2156(08)70264-3.
- [25] J.P. Hirth and J. Lothe. *Theory of Dislocations*. Wiley, New York, 1982.
- [26] A. Hmiel, J. M. Winey, Y. M. Gupta, and M. P. Desjarlais. Nonlinear elastic response of strong solids: First-principles calculations of the third-order elastic constants of diamond. *Physical Review B*, 93:174113, May 2016. doi: 10.1103/PhysRevB.93.174113.

- [27] M.J. Horodon and B.L. Averbach. Precision density measurements on deformed copper and aluminum single crystals. *Acta Metallurgica*, 9:247–249, 1961. doi: 10.1016/0001-6160(61)90074-8.
- [28] D. S. Hughes and J. L. Kelly. Second-order elastic deformation of solids. *Physical Review*, 92:1145–1149, Dec 1953. doi: 10.1103/PhysRev.92.1145.
- [29] A.S. Johal and D.J. Dunstan. Reappraisal of experimental values of third-order elastic constants of some cubic semiconductors and metals. *Physical Review B*, 73:024106, Jan 2006. doi: 10.1103/PhysRevB.73.024106.
- [30] S. Jones and Ch.S. Menon. Non-linear elastic behavior of hexagonal silicon carbide. *physica status solidi (b)*, 251(6):1186–1191, 2014. ISSN 1521-3951. doi: 10.1002/pssb.201451024.
- [31] G. Jurczak and P. Dłużewski. Finite element modelling of nonlinear piezoelectricity in wurtzite GaN/AlN quantum dots. *Computational Materials Science*, 111:197–202, 2016. ISSN 0927-0256. doi: 10.1016/j.commatsci.2015.09.024.
- [32] G. Jurczak and P. Dłużewski. Finite element modelling of threading dislocation effect on polar GaN/AlN quantum dot. *Physica E: Low-dimensional Systems and Nanostructures*, 95:11–15, 2018. ISSN 1386-9477. doi: 10.1016/j.physe.2017.08.018.
- [33] J.M. Lang and Y.M. Gupta. Experimental determination of third-order elastic constants of diamond. *Physical Review Letters*, 106:125502, Mar 2011. doi: 10.1103/PhysRevLett.106.125502.
- [34] S.P. Łepkowski. Significance of third-order elasticity for determination of the pressure coefficient of the light emission in strained quantum wells. *Physical Review B*, 78:153307, Oct 2008. doi: 10.1103/PhysRevB.78.153307.
- [35] M. Łopuszyński and J.A. Majewski. Ab initio calculations of third-order elastic constants and related properties for selected semiconductors. *Physical Review B*, 76:045202, Jul 2007. doi: 10.1103/PhysRevB.76.045202.
- [36] M. Maździarz. Unified isoparametric 3D lagrange finite elements. *Computer Modeling in Engineering & Sciences*, 66(1):1–24, 2010. doi: 10.3970/cmesc.2010.066.001.
- [37] M. Maździarz and M. Gajewski. Estimation of isotropic hyperelasticity constitutive models to approximate the atomistic simulation data for aluminium and tungsten monocrystals. *Computer Modeling in Engineering & Sciences*, 105(2):123–150, 2015. doi: 10.3970/cmesc.2015.105.123.
- [38] H.J. McSkimin and P. Andreatch Jr. Elastic moduli of diamond as a function of pressure and temperature. *Journal of Applied Physics*, 43(7):2944–2948, 1972. doi: 10.1063/1.1661636.
- [39] A. Menzel and P. Steinmann. On the comparison of two strategies to formulate orthotropic hyperelasticity. *Journal of Elasticity*, 62:171201, 2001. doi: 10.1023/A:101293750.
- [40] C. Miehe. Comparison of two algorithms for the computation of fourth-order isotropic tensor functions. *Computers & Structures*, 66:37–13, 1998. doi: 10.1016/S0045-7949(97)00073-4.
- [41] F. D. Murnaghan. Finite deformations of an elastic solid. *American Journal of Mathematics*, 59(2):235–260, 1937. ISSN 00029327. doi: 10.2307/2371405.
- [42] O. H. Nielsen. Optical phonons and elasticity of diamond at megabar stresses. *Physical Review B*, 34:5808–5819, Oct 1986. doi: 10.1103/PhysRevB.34.5808.
- [43] Andrew N. Norris. Higher derivatives and the inverse derivative of a tensor-valued function of a tensor. *Quart. Appl. Math.*, 66(4):725–741, 2008. doi: 10.1090/S0033-569X-08-01108-2.
- [44] R. W. Ogden. *Non-Linear Elastic Deformations*. Ellis Horwood Ltd., Chichester, 1984.
- [45] J.-P Poirier and A. Tarantola. A logarithmic equation of state. *Physics of the Earth and Planetary Interiors*, 109(12):1 – 8, 1998. ISSN 0031-9201. doi: 10.1016/S0031-9201(98)00112-5.
- [46] R. E. Schramm. Ultrasonic measurement of stress in railroad wheels. *Review of Scientific Instruments*, 70(2): 1468–1472, 1999. doi: 10.1063/1.1149607.

- [47] B. R. Seth. Generalized strain measure with applications to physical problems. In M. Reiner and D. Abir, editors, *Second-Order Effects in Elasticity, Plasticity and Fluid Dynamics, Proceedings of International Symposium, Haifa, April 23-27, 1962*, pages 162–172, Oxford, 1964. Pergamon Press.
- [48] D. Singh, D.K. Pandey, D.K. Singh, and R.R. Yadav. Propagation of ultrasonic waves in neptunium monochalcogenides. *Applied Acoustics*, 72(10):737 – 741, 2011. ISSN 0003-682X. doi: 10.1016/j.apacoust.2011.04.002.
- [49] R. K. Singh, R. P. Singh, and M. P. Singh. Acoustical characterization of nanostructured metals. *International Journal of Nanoscience*, 07(06):315–323, 2008. doi: 10.1142/S0219581X08005481.
- [50] F. Spaepen. Interfaces and stresses in thin films. *Acta Materialia*, 48:31–42, 2000. doi: 10.1016/S1359-6454(99)00286-4.
- [51] R. N. Thurston and K. Brugger. Third-order elastic constants and the velocity of small amplitude elastic waves in homogeneously stressed media. *Physical Review*, 133(6A):1604–1610, 1964. doi: 10.1103/PhysRev.135.AB3.2.
- [52] R. N. Thurston, H. J. McSkimin, and P. Andreatch. Third-order elastic coefficients of quartz. *Journal of Applied Physics*, 37(1):267–275, 1966. doi: 10.1063/1.1707824.
- [53] N. J. Walker, G. A. Saunders, and J. E. Hawkey. Soft TA models and anharmonicity in cadmium telluride. *Philosophical Magazine B*, 52(5):1005–1018, 1985. doi: 10.1080/01418638508241890.
- [54] Duane C. Wallace. Thermoelastic theory of stressed crystals and higher-order elastic constants. *Solid State Physics*, 25:301 – 404, 1970. ISSN 0081-1947. doi: 10.1016/S0081-1947(08)60010-7.
- [55] Hao Wang and Mo Li. *Ab initio* calculations of second-, third-, and fourth-order elastic constants for single crystals. *Physical Review B*, 79:224102, Jun 2009. doi: 10.1103/PhysRevB.79.224102.
- [56] Rui Wang, Shaofeng Wang, Xiaozhi Wu, Yin Yao, and Anping Liu. *Ab initio* calculations on the third-order elastic constants for selected B2MgRE (RE=Y, Tb, Dy, Nd) intermetallics. *Intermetallics*, 18(12):2472 – 2476, 2010. ISSN 0966-9795. doi: 10.1016/j.intermet.2010.08.039.
- [57] X. Wang, Y. Gu, Xu Sun, and Yue Zhang. Nonlinear elastic response of cubic crystals to biaxial strain. *Computational Materials Science*, 79(0):284 – 288, 2013. ISSN 0927-0256. doi: 10.1016/j.commatsci.2013.05.058.
- [58] J.M. Winey, A. Hmiel, and Y.M. Gupta. Third-order elastic constants of diamond determined from experimental data. *Journal of Physics and Chemistry of Solids*, 93:118–120, 2016. ISSN 0022-3697. doi: 10.1016/j.jpcs.2016.02.016.
- [59] T.D Young, J. Kioseoglou, G.P. Dimitrakopoulos, P. Dłuzewski, and Ph. Komninou. 3D modelling of misfit networks in the interface region of heterostructures. *Journal of Physics D: Applied Physics*, 40(13):4084, 2007. doi: 10.1088/0022-3727/40/13/027.
- [60] J. Zhao, J.M. Winey, and Y.M. Gupta. First-principles calculations of second- and third-order elastic constants for single crystals of arbitrary symmetry. *Physical Review B*, 75:094105, Mar 2007. doi: 10.1103/PhysRevB.75.094105.

A Appendix

For isoparametric FEs the substitution of (45) into $\mathbf{K}_{mn} \stackrel{df}{=} \frac{\partial \mathbf{P}_m}{\partial \mathbf{a}_n}$ can be rewritten in the following form

$$K_m^i n^j = \int_V \left(\frac{\partial \hat{\mathcal{E}}_{PR}}{\partial a_{mi}} \frac{\partial \hat{\mathcal{G}}^{PR}}{\partial \hat{\mathcal{E}}_{ST}} \frac{\partial \hat{\mathcal{E}}_{ST}}{\partial a_{nj}} + \hat{\mathcal{G}}^{PR} \frac{\partial^2 \hat{\mathcal{E}}_{PR}}{\partial a_{mi} \partial a_{nj}} \right) \det \mathbf{F}^{-1} dv. \quad (47)$$

$\frac{\partial^2 \hat{\mathcal{E}}}{\partial \mathbf{a}_m \partial \mathbf{a}_n}$ can be considered as the second derivative of a complex tensor function $\hat{\mathcal{E}} = \hat{\mathcal{E}}(\mathbf{E})$, where the Green strain depends on nodal displacement vectors, $\mathbf{E} = \mathbf{E}(\mathbf{a}_1, \dots, \mathbf{a}_k)$. According to the chain rule this derivative reads

$$\frac{\partial^2 \hat{\mathcal{E}}_{PR}}{\partial a_{mi} \partial a_{nj}} = \frac{\partial \hat{\mathcal{E}}_{PR}}{\partial E_{ST}} \frac{\partial^2 E_{ST}}{\partial a_{mi} \partial a_{nj}} + \frac{\partial^2 \hat{\mathcal{E}}_{PR}}{\partial E_{ST} \partial E_{MN}} \frac{\partial E_{ST}}{\partial a_{mi}} \frac{\partial E_{MN}}{\partial a_{nj}}, \quad (48)$$

where

$$\frac{\partial E_{KL}}{\partial a_{mi}} = \frac{1}{2}(N_{mi,K}F^i{}_L + N_{mi,L}F^i{}_K), \quad \frac{\partial^2 E_{KL}}{\partial a_{mi} \partial a_{nj}} = g^{ij}N_{mi,K}N_{nj,L}, \quad \frac{\partial^3 E_{KL}}{\partial a_{mi} \partial a_{nj} \partial a_{ab}} = 0. \quad (49)$$

Substitution of (49) into (48), and the following result into (47) gives subsequently

$$\begin{aligned} K_m^i n^j &= \int_V \left(\frac{1}{2}(g^i{}_p N_{mi,r} + g^i{}_r N_{mi,p}) \mathcal{A}_{PR}{}^{pr} \frac{\partial \widehat{\mathcal{G}}^{PR}}{\partial \widehat{\mathcal{E}}_{ST}} \mathcal{A}_{ST}{}^{st} \frac{1}{2}(g^j{}_s N_{mj,t} + g^j{}_t N_{mj,s}) \right. \\ &\quad \left. + \frac{1}{2}(N_{mi,S}F^i{}_T + N_{ni,T}F^i{}_S) \widehat{\mathcal{G}}^{PR} \frac{\partial^2 \widehat{\mathcal{E}}_{PR}}{\partial E_{ST} \partial E_{KL}} \frac{1}{2}(N_{mj,K}F^j{}_L + N_{nj,L}F^j{}_K) \right. \\ &\quad \left. + g^{ij}N_{mi,S}N_{mj,T} \frac{\partial \widehat{\mathcal{E}}_{PR}}{\partial E_{ST}} \widehat{\mathcal{G}}^{PR} \right) \det \mathbf{F}^{-1} dv \\ &= \int_V N_{mi,k} \left[\left(\mathcal{A}_{PR}{}^{ik} \frac{\partial \widehat{\mathcal{G}}^{PR}}{\partial \widehat{\mathcal{E}}_{ST}} \mathcal{A}_{ST}{}^{jl} + \widehat{\mathcal{G}}^{PR} F^i{}_S F^k{}_T \frac{\partial^2 \widehat{\mathcal{E}}_{PR}}{\partial E_{ST} E_{MN}} F^j{}_M F^l{}_N \right) \det \mathbf{F}^{-1} + g^{ij} \sigma^{kl} \right] N_{nj,l} dv. \end{aligned} \quad (50)$$

The last term leads to (46) where $\mathcal{B}_{PR}{}^{ijkl} = F^i{}_I F^k{}_K F^j{}_J F^l{}_L \frac{\partial^2 \widehat{\mathcal{E}}_{PR}}{\partial E_{IJ} \partial E_{KL}}$. According to (24) the second derivative $\frac{\partial^2 \widehat{\mathcal{E}}}{\partial \mathbf{E}^2}$ rewritten in the stretch eigenvector basis reads

$$\frac{\partial^2 \widehat{\mathcal{E}}^{ij}}{\partial E_j \partial E_k} = \begin{cases} u_i^4 \varepsilon''(E_i) & \text{for } u_i = u_j = u_k, \\ 2u_i u_j^3 \frac{\varepsilon(E_j) - \varepsilon(E_i)}{E_j - E_i} - \varepsilon'(E_k) & \text{for } u_i \neq u_j = u_k, \\ -2u_i u_j u_k^2 \frac{\varepsilon(E_i)(E_j - E_k) + \varepsilon(E_j)(E_k - E_i) + \varepsilon(E_k)(E_i - E_j)}{(E_i - E_j)(E_j - E_k)(E_k - E_i)} & \text{for } u_i \neq u_j \neq u_k \neq u_i, \end{cases} \quad (51)$$

where

$$E_i = \frac{1}{2}(u_i^2 - 1), \quad (52a)$$

$$\widehat{\varepsilon}(E_i) = f(u_i), \quad (52b)$$

$$\widehat{\varepsilon}'(E_i) = \frac{\partial f(u_i(E_i))}{\partial E_i} = \frac{\partial f}{\partial u_i} \frac{\partial u_i}{\partial E_i} = u_i^{-1} f'(u_i), \quad (52c)$$

$$\widehat{\varepsilon}''(E_i) = \frac{\partial^2 f}{\partial E_i^2} = \frac{\partial}{\partial E_i} \left(\frac{\partial f}{\partial E_i} \right) = \frac{\partial}{\partial u_i} \left(\frac{\partial f}{\partial u_i} \frac{\partial u_i}{\partial E_i} \right) \frac{\partial u_i}{\partial E_i} = u_i^{-2} f''(u_i) - u_i^{-3} f'(u_i). \quad (52d)$$